Ceria Catalysis

International Edition: DOI: 10.1002/anie.201510903
German Edition: DOI: 10.1002/ange.201510903

Oxychlorination–Dehydrochlorination Chemistry on Bifunctional Ceria Catalysts for Intensified Vinyl Chloride Production

*Matthias Scharfe, Pedro A. Lira-Parada, Vladimir Paunović, Maximilian Moser, Amol P. Amrute, and Javier Pérez-Ramírez**

Abstract: *Ceria catalyzes the one-step production of the vinyl chloride monomer (VCM) from ethylene with a high yield because of its bifunctional character: redox centers oxychlorinate ethylene to ethylene dichloride (EDC), which is subsequently dehydrochlorinated to VCM over strong acid sites generated in situ. Nanocrystalline CeO_2 and CeO_2-ZrO_2 lead to a VCM yield of 25 % in a single pass, outperforming the best reported systems and reaching industrially attractive levels. The use of CeO_2 intensifies the current two-step process within PVC production encompassing $CuCl_2$-catalyzed oxychlorination and thermal cracking. In addition, ceria-based materials offer stability advantages with respect to the archetypical $CuCl_2$-based catalysts.*

The development of more efficient and sustainable manufacturing technologies relies on the discovery of multifunctional catalytic materials and novel reaction concepts. Once established in industry, catalysts and corresponding processes are optimized often over decades, but extensive changes in the original catalyst formulation or disruptive decisions to opt for radical new routes are rarely made. Within the polyvinyl chloride (PVC) manufacturing industry (44 Mton per year),[1] vinyl chloride (VCM), produced by means of a two-step process, is an example of this. The process involves ethylene oxychlorination to ethylene dichloride (EDC), followed by thermal cracking of EDC to form VCM (Figure 1). In the 1950s, the production of VCM was first intensified through the implementation of ethylene oxychlorination to close the chlorine loop by recycling the by-product HCl, produced in the thermal cracking stage. Still today, the oxychlorination reaction relies on the use of $CuCl_2$-based catalysts, inherited from the Deacon reaction (HCl oxidation),[2a] attaining practically full selectivity to EDC at 473–513 K.[1a] Although this catalyst was abandoned in the Deacon reaction because of its insufficient durability,[2a] it is still applied in the oxychlorination reaction firstly because of the lower operating temperature, and secondly as a result of the tremendous efforts that have been directed towards its stabilization through doping.[3] However, stability issues, including: 1) volatilization of the copper phase linked to the inevitable formation of hot spots in fixed bed operation and 2) particle agglomeration (widely known as stickiness)[2] in fluidized bed operation, are yet unresolved. Moreover, owing to high operating temperature of the thermal cracking (773–823 K),[1] the integration of the two processes in one step is not feasible since this would further compromise the stability of the copper-based catalyst.[4] Efforts to address this using non-copper-containing materials, such as lanthanum (oxy)chloride, have been made previously, however the VCM yields achieved, compared to the two-step process, were substantially lower.[5]

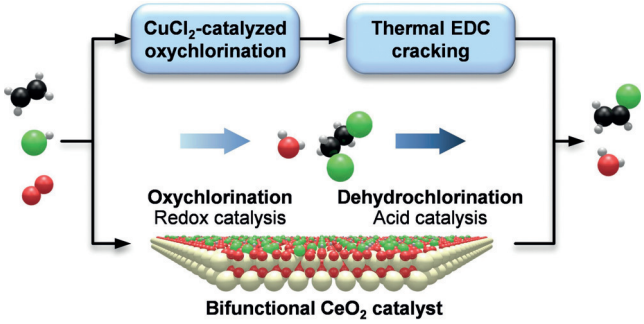

Figure 1. Top: The current two-step process for VCM production, encompassing $CuCl_2$-catalyzed oxychlorination and thermal EDC cracking. The first step involves active-metal volatilization and particle agglomeration, whereas the second step is unselective and energy intensive, leading to a VCM yield of circa 50%. Bottom: The bifunctional ceria catalyst developed in this work integrates both oxychlorination and dehydrochlorination processes on a single surface, thereby leading to intensified VCM production. Atom colors: C = black; Cl = green; O = red; H = light gray; Ce = pale yellow.

In the present work, our results show a solid basis for a new wave of process intensification by identifying a novel catalyst enabling the stable production of VCM from ethylene in one step. For the first time, we have found that cerium oxide not only exhibits exceptional redox properties that can be moderated, but also features acid sites under oxychlorination conditions that promote the dehydrochlorination of EDC. The interaction of redox and acid centers on this bifunctional material enables the integration of oxychlorination and dehydrochlorination on a single surface (Figure 1).

Our choice to investigate certain oxides in the oxychlorination process is justified by our studies on HCl oxidation, which demonstrated that oxide-based systems, particularly IrO_2, RuO_2, and CeO_2, are outstandingly stable and active compared to traditional $CuCl_2$-based catalysts.[6] The strong oxidative character of these oxides, which might lead to the over-oxidation of ethylene, can be anticipated to be altered

[*] M. Scharfe, P. A. Lira-Parada, V. Paunović, M. Moser, Dr. A. P. Amrute, Prof. J. Pérez-Ramírez
Institute for Chemical and Bioengineering
Department of Chemistry and Applied Biosciences, ETH Zurich
Vladimir-Prelog-Weg 1, 8093 Zurich (Switzerland)
E-mail: jpr@chem.ethz.ch

Supporting information for this article is available on the WWW under http://dx.doi.org/10.1002/anie.201510903.

under oxychlorination conditions.[6] The $CuCl_2$-based benchmark catalyst was also evaluated under its optimized conditions[1a] to compare its performance to that of the oxides. Catalytic tests in a continuous-flow fixed-bed reactor (see Figure S1 in the Supporting Information) revealed circa 10% C_2H_4 conversion and full selectivity to EDC over the benchmark system (Figure 2a). In contrast, IrO_2 and RuO_2 resulted mostly in over-oxidation of ethylene to CO and CO_2. However, the oxychlorination tests on CeO_2-1173 (the calcination temperature of ceria is 1173 K) unveiled an outstanding catalytic behavior, leading to a similar C_2H_4 conversion level of circa 13% and selectivity to the desired chlorinated products of 98% (92% EDC, 6% VCM) and to CO of only 2%. The high selectivity to chlorinated products was also maintained at elevated temperature as applied for other oxides (Figure S2). Under these conditions 35% of C_2H_4 conversion was obtained with 85% EDC and 13% VCM selectivities.

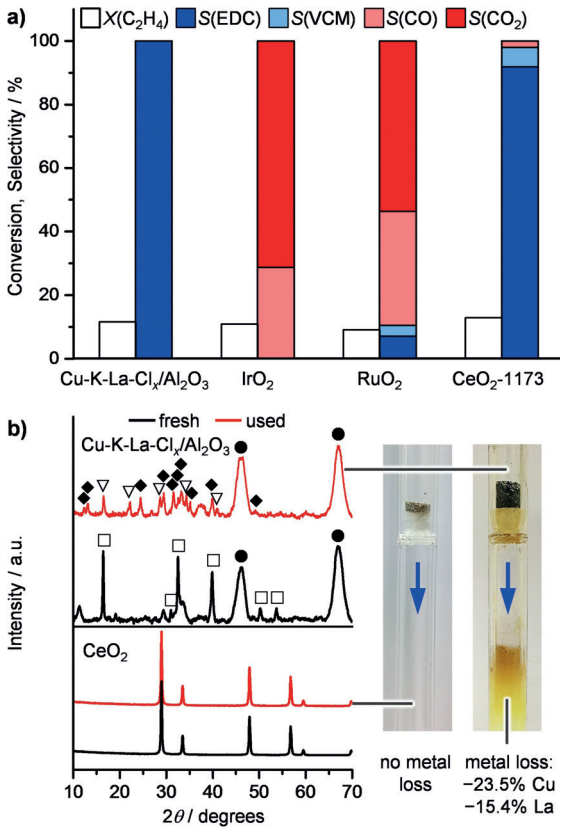

Figure 2. a) C_2H_4 conversion (X) and product selectivity (S) over IrO_2 and RuO_2 at 673 K, CeO_2-1173 at 623 K, and Cu-K-La-Cl_x/Al_2O_3 at 473 K. Conditions: $W_{cat}=0.5$ g; $F_T=100$ cm^3 STP min^{-1} containing 3 vol.% C_2H_4, 4.8 vol.% HCl, and 1.2 vol.% O_2 (3 vol.% for CeO_2-1173) balanced in He; $P=1$ bar. b) X-ray diffractograms of Cu-K-La-Cl_x/Al_2O_3 and CeO_2-1173 samples in the fresh form and after temperature cycles (Figure S4). Both fresh and used ceria samples display a pure CeO_2 phase, with no deposits on the reactor wall or supporting quartz wool. The crystalline phases identified in the $CuCl_2$-based sample change strongly upon reaction and deposits of volatilized metal species are visible on the reactor wall. The symbols ●, □, ▽, and ◆ denote reflections attributed to γ-Al_2O_3 (JCPDS 48-0367), $Cu_2(OH)_3Cl$ (JCPDS 70-0821), $CuCl_2{\cdot}2H_2O$ (JCPDS 71-2288), and $KCl{\cdot}CuCl_2$ (JCPDS 20-0874), respectively. Arrows on the reactors indicate the flow direction.

The exceptional resistance of ceria towards combustion can be traced back to its oxidation reactivity under chlorinating conditions. We have previously established that under chlorinating conditions, the oxidation of CO is practically suppressed over ceria, whereas IrO_2 and RuO_2 under the same conditions still oxidized CO to CO_2 at slightly higher temperatures.[6c] In addition, C_2H_4 oxidation tests conducted under the oxychlorination conditions evidenced that CeO_2 led to low C_2H_4 conversion (12%) at 673 K, whereas IrO_2 and RuO_2 showed circa 40% conversion already at 523 K and 573 K, respectively (Figure S3). This clearly substantiates the over-oxidation of ethylene over IrO_2 and RuO_2 compared to the negligible formation of CO on CeO_2 in the oxychlorination reaction.

Contrasting the performance of CeO_2 with the Cu-based benchmark catalyst, it can be seen that CeO_2 leads to a circa four times higher overall yield of chlorinated products. Furthermore, the most exciting results come from a comparison of their stabilities using temperature cycling experiments (Figure 2b; Figures S4–6), which simulate the stress a catalyst undergoes in an exothermic large-scale fixed-bed reactor process where temperature fluctuations can be anticipated.[2] Overall, the reactivity of both the catalysts remained unaltered (Figure S4). However, the inspection of reactors and the analysis of samples post-reaction pointed to significant differences. CeO_2-1173 preserved its crystallinity and did not show any sign of metal loss upon reaction, as can be seen from the clean reactor (Figure 2b; Figure S5, Table S1). In-depth analysis by high-resolution TEM images of the samples before and after temperature cycles showed that the crystallinity and the morphology of ceria remained intact, in line with its remarkably stable performance during the temperature cycles and in an additional isothermal stability test over 10 h on stream at 673 K (Figure S5, Figure S2). In contrast, the benchmark catalyst exhibited substantial structural and textural alterations upon use and most importantly a severe metal loss. The metal loss is evidenced by the transformation and reduction of the intensity of phases attributable to Cu in the X-ray diffractograms, as well as by the colored deposits visible on the reactor wall (Figure 2b). These results are further confirmed by X-ray fluorescence (XRF) analysis and unequivocally suggest the superior robustness of CeO_2 compared to the $CuCl_2$-based benchmark system for the oxychlorination of ethylene.

A further striking feature of CeO_2 was the formation of considerable amounts of VCM occurring already at 673 K, which is 100–150 K lower than the thermal EDC cracking temperature (see above).[1a] This result suggests the catalytic production of VCM on CeO_2. The formation of VCM was proposed as a source of over-chlorinated products over $CuCl_2$-based catalysts.[2e] However, we have not detected such undesirable chlorinated products over CeO_2-1173, as confirmed by the retention-time experiments shown in Figure S7. It should be emphasized that previous efforts in this direction have been futile so far, being challenged by low VCM yields[5] or the formation of combustion products, as seen in the case of RuO_2 (Figure 2a). LaOCl, which has been

reported previously to produce VCM with high selectivity,[5] was virtually inactive under the operating conditions of CeO_2. Therefore, the VCM formation on CeO_2 was further investigated. First, to ascertain whether the VCM generation occurs simultaneously with EDC or successively from EDC dehydrochlorination, the oxychlorination of ethylene was performed at variable residence time (Figure 3a). Upon increasing the residence time, C_2H_4 conversion increased as expected, however the selectivity to EDC decreased and that to VCM increased. If the two reactions leading to EDC and VCM were independent, the ratio of EDC to VCM would remain constant. The fact that this ratio did change upon varying the residence time explicitly suggests that the two processes occur consecutively. Second, the EDC dehydrochlorination behavior of CeO_2 was compared with that of thermal cracking. Figure 3b displays the VCM yield obtained by feeding EDC with or without O_2 and/or HCl over CeO_2-1173 or quartz particles (employed as an inert material to allow the same contact time as for CeO_2-1173). When only EDC in He gas was fed into the system, ceria behaved similarly to quartz with no VCM formation up to 723 K. Introduction of O_2 and HCl separately led to EDC dehydrochlorination on CeO_2 at 623 K, reaching circa 60% VCM yield at 723 K. With simultaneous feeding of both HCl and O_2 with EDC, like in the case of oxychlorination reaction, the EDC cracking performance was further shifted to lower temperature by circa 100 K over CeO_2, leading to a VCM yield of circa 90% at 673 K. Thus, it appears that the reaction feed modifies the surface properties of CeO_2, which catalyzes the dehydrochlorination of EDC to VCM.

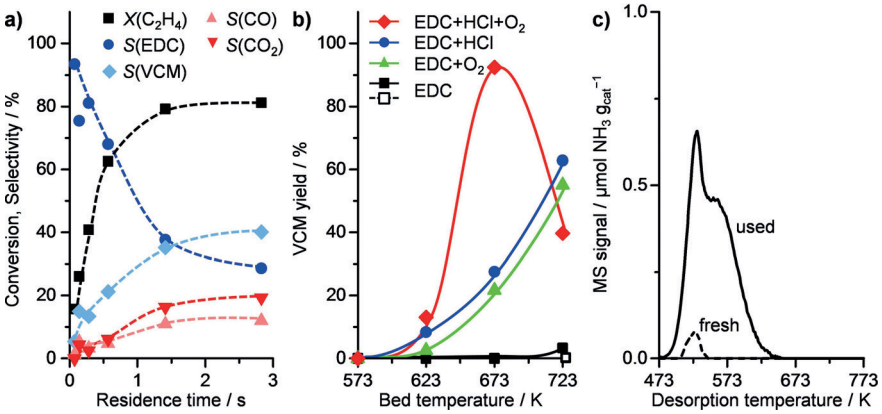

Figure 3. a) Impact of residence time (W_{cat} = 0.25–10 g) on C_2H_4 conversion and product distribution over CeO_2-1173 at 673 K and with a ratio of C_2H_4/HCl/O_2 = 3:4.8:3. b) VCM yield versus bed temperature in the dehydrochlorination of EDC with or without addition of O_2 (3 vol.%) and/or HCl (4.8 vol.%) over 0.5 g of CeO_2-1173 (solid symbols) and quartz (open symbols). Other conditions: F_T = 100 cm^3 STP min^{-1}, P = 1 bar. c) Temperature-programmed desorption of NH_3 over CeO_2-1173 in its fresh form and after use in ethylene oxychlorination.

It is known that both Lewis and Brønsted acid sites play a crucial role in the transformation of EDC to VCM.[7] Thus, we characterized fresh and post-reaction samples by temperature-programmed desorption of NH_3 (NH_3-TPD; Figure 3c, Table S2). Fresh CeO_2-1173 displayed very low NH_3 desorption (2 µmol NH_3 g^{-1}) at lower temperature (< 550 K), which is consistent with the absence of dehydrochlorination activity when solely EDC was fed. The sample after the oxychlorination of ethylene showed a huge increase in the NH_3 desorption (31 µmol NH_3 g^{-1}) at lower temperature and led to an additional peak (21 µmol NH_3 g^{-1}) at slightly higher temperature (circa 570 K). These results suggest that new acid sites are generated on the CeO_2 surface. These sites might be composed of surface hydroxy groups formed by hydrogen abstraction from HCl or a vacancy generated as a result of the removal of surface chlorine-containing species and/or evolution of H_2O.[6a,8] With regards to the oxychlorination of ethylene to EDC, it is suggested, based on previous studies, that the redox character of CeO_2 is key to catalyze the EDC formation.[6a] Thus, ceria features both redox and acid sites on its surface, enabling conversion of ethylene into VCM in one step.

Our next step was to improve the VCM fraction, while minimizing that of CO_x. As a first approach, we studied the effect of reaction parameters on the C_2H_4 conversion and product distribution. Upon raising the bed temperature, both the C_2H_4 conversion and selectivity to VCM were increased. However, higher temperatures also caused a higher degree of combustion forming CO and CO_2 (Figure 4a). Variation of O_2 and HCl feed contents separately resulted in a steady increase in conversion, likely because of the higher availability of the reactants facilitating the re-oxidation of the catalyst surface as detected in the case of HCl oxidation (Figure 4b,c).[6a] Notably, the CO_x fraction was low in the case of O_2 variation and it was substantially decreased at higher HCl concentrations, however the selectivity to VCM remained almost unaltered in both cases. At the same time, the high HCl content seems to be beneficial to boost EDC selectivity as a result of the curtailed combustion, but the reaction parameters generally had little impact on the dehydrochlorination of EDC to VCM.

Next, we investigated the impact of the material properties on VCM production. Commercial ceria was calcined at different temperatures, leading to materials with different crystallinities and specific surface areas (Table S1), and was tested in the oxychlorination reaction. The VCM yield increased linearly with increasing total surface area of the samples (Figure 4d). Likewise, the VCM-to-EDC ratio also increased, highlighting a drop in EDC fraction resulting from its dehydrochlorination to VCM (Figure 4e). However, the high-surface-area materials obtained by calcining commercial ceria at lower temperatures than 1173 K underwent sintering and a drop in the specific surface area which significantly decreased the VCM yield and VCM-to-EDC ratio after 8 h on stream (Figure 4d,e open data points; Figure S2). Thus, we opted for a synthetic method which has been established to

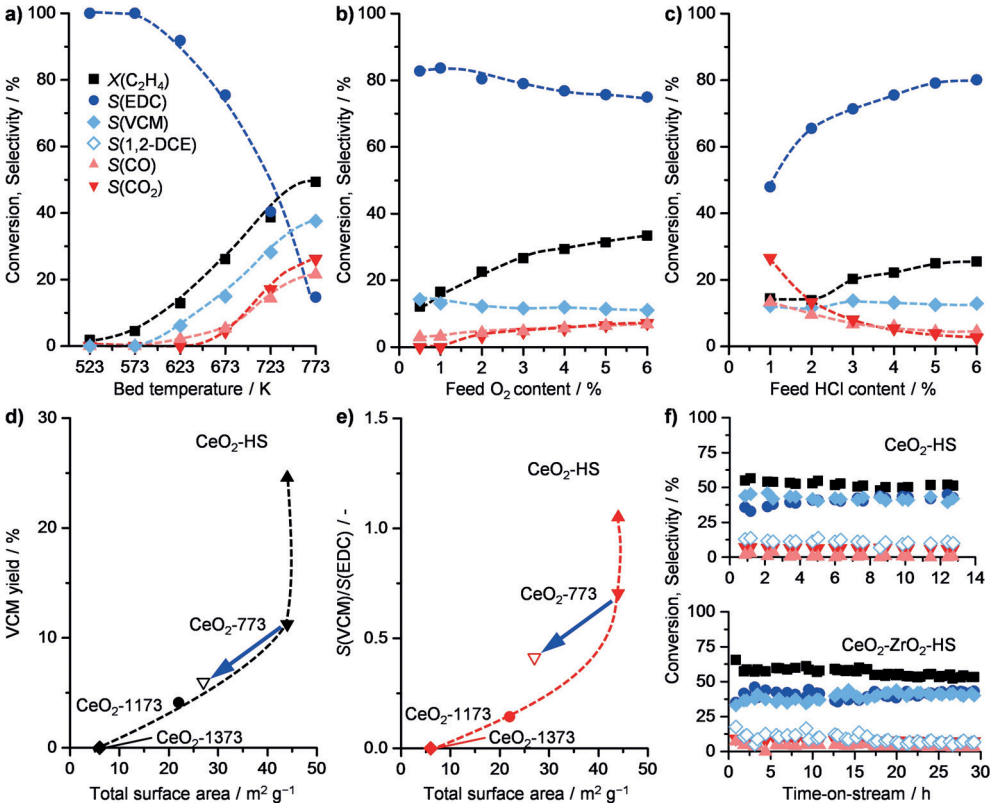

Figure 4. Influence of a–c) reaction parameters and d–f) the properties of the catalyst on C_2H_4 conversion and product distribution. Plots (a–c) show C_2H_4 conversion and product selectivity versus a) bed temperature, b) feed O_2 content at fixed HCl (4.8 vol.%) and C_2H_4 (3 vol.%) concentrations, and c) feed HCl content at fixed O_2 (3 vol.%) and C_2H_4 (3 vol.%) concentrations over CeO_2-1173. d) VCM yield and e) VCM-to-EDC ratio versus total surface area of CeO_2 samples. f) C_2H_4 conversion and product selectivity versus time-on-stream over CeO_2-HS and CeO_2-ZrO_2-HS. Conditions: $W_{cat}=0.5$ g, $T_{bed}=673$ K (b–f), ratio of $C_2H_4/HCl/O_2=3:4.8:3$ (a, d–f), $F_T=100\ cm^3\ STP\ min^{-1}$, $P=1$ bar.

preserve the high surface area of CeO_2 under harsh conditions.[9] The method involves hydrolysis of cerium nitrate at room temperature using H_2O_2 and NH_4OH, followed by drying and calcination steps. This sample (CeO_2-HS) exhibited an unprecedented VCM yield, which outpaced the surface area relationship (24%; Figure 4d), and maintained a stable performance for more than 10 h on stream (Figure 4f, top). However, in this case 1,2-dichloroethylene (1,2-DCE) was produced with 10% selectivity, likely as a result of larger quantity of acid sites (see below). The VCM-to-EDC ratio was unity, suggesting that circa 50% of the total EDC produced is converted into VCM on the CeO_2-HS surface, which is comparable to the VCM yield attained in thermal EDC cracking (Figure 1).[1a]

Inspired by these results and by the known activity promotion detected in HCl and HBr oxidation when ceria is homogeneously mixed with ZrO_2, we prepared a high-surface-area CeO_2-ZrO_2 (CeO_2-ZrO_2-HS) catalyst using the above-mentioned procedure. For this material, an improved C_2H_4 conversion of more than 60% was obtained and high selectivities to the desired products were maintained for more than 30 h on stream (Figure 4f, bottom), highlighting the superb robustness of the system. Overall, CeO_2-based systems achieved approximately 30% VCM yield at a contact time of only 0.14 s, which is much higher than that reported for ethylene-to-VCM transformation on lanthanum-based systems (11–18%) at a contact time of 3.6–8.7 s.[5]

To shed light on the remarkable dehydrochlorination activity of the high-surface-area samples, we characterized their fresh and used forms (Figure S8; Table S1,2). As expected, the surface area of these materials was largely unchanged with respect to their fresh analogues. However, the acidity analysis presented intriguing differences. Fresh systems exhibited a lower amount of weak acid sites, whereas the used systems revealed higher numbers of weak acid sites and the generation of new stronger acid sites (centered at 593 K) on CeO_2-HS. The total concentration of acid sites on CeO_2-HS (109 $\mu mol\ NH_3\ g^{-1}$) was twice that of CeO_2-1173, however the VCM selectivity on CeO_2-HS was circa fourfold higher than that of CeO_2-1173. Thus, it seems that not all acid sites are responsible for EDC dehydrochlorination. In fact, the VCM selectivity appears to correlate with the quantity of stronger acid centers (i.e. NH_3 desorption above 550 K), which is circa four times higher on CeO_2-HS than on CeO_2-1173. CeO_2-ZrO_2-HS also formed a large amount of new acid sites (93 $\mu mol\ NH_3\ g^{-1}$) compared to its fresh form (9 $\mu mol\ NH_3\ g^{-1}$), however these sites are much stronger (centered at 685 K) than those on CeO_2-1173 and CeO_2-HS. Thus, it appears that different initial properties of ceria lead to acid sites with different strengths. However, sites which can be probed by NH_3 desorption above 550 K are effective for the dehydrochlorination of EDC.

In summary, we have demonstrated highly efficient oxychlorination–dehydrochlorination chemistry on ceria-based catalysts for the production of vinyl chloride. Nanocrystalline ceria-based samples exhibited stable ethylene conversions and high selectivities to VCM, outperforming the best reported systems and reaching industrially attractive levels. The remarkable stability of ceria was proven by isothermal and temperature cycling experiments, showing neither activity loss nor material degradation. We believe that our findings will have significant impact on the intensification of the current two-step process within PVC production involving $CuCl_2$-catalyzed oxychlorination and thermal cracking.

Experimental Section

Details on catalyst preparation, characterization, and testing are provided in the Supporting Information. Briefly, we have investigated commercial RuO_2 and CeO_2, the latter calcined at temperatures in the range of 773–1373 K (coded CeO_2–x, where x is the calcination temperature in K). IrO_2 was prepared by thermal decomposition of $IrCl_3$ at 773 K in static air. High-surface-area nanocrystalline ceria (CeO_2-HS) and ceria–zirconia (Ce:Zr = 3) mixed oxide (CeO_2-ZrO_2-HS) were synthesized by (co)precipitation of the precursor salts using H_2O_2 and NH_4OH, followed by drying and calcination at 773 K.[9] A benchmark copper-based oxychlorination catalyst, denoted Cu-K-La-Cl_x/Al_2O_3 (containing 7 wt.% Cu, 2 wt.% K, and 2 wt.% La), was prepared by sequential incipient wetness impregnation of γ-Al_2O_3 with the corresponding metal chlorides following a method reported in the patent literature.[3] The oxychlorination of ethylene was studied at atmospheric pressure and temperatures (T_{bed}) of 473–773 K in a continuous-flow fixed-bed quartz microreactor set-up (Figure S1) using a catalyst mass (W_{cat}) of 0.5–10 g (particle size d_P = 0.4–0.6 mm) and a total gas flow (F_T) of 100 cm^3 STP min^{-1} containing 3 vol.% C_2H_4, 1–6 vol.% HCl, and 0.5–6 vol.% O_2 balanced in He. The gas composition at the reactor outlet was analyzed online using a gas chromatograph coupled to a mass spectrometer. The fresh and used catalysts were characterized by X-ray diffraction, X-ray fluorescence, N_2 sorption, temperature-programmed desorption of NH_3, and electron microscopy.

Acknowledgements

This work was supported by the Swiss National Science Foundation (project no. 2-77204-14). We thank ScopeM and Dr. Sharon Mitchell for the microscopic analyses.

Keywords: cerium oxide · heterogeneous catalysis · industrial chemistry · oxychlorination · vinyl chloride

How to cite: *Angew. Chem. Int. Ed.* **2016**, *55*, 3068–3072
Angew. Chem. **2016**, *128*, 3120–3124

[1] a) J. S. Naworski, E. S. Velez, *Applied Industrial Catalysis*, *Vol. 1* (Ed.: B. E. Leach), Academic Press, New York, **1983**, pp. 239–273; b) Renolit press release, 2015. Everything about PVC from manufacturing to recycling, www.renolit.com, accessed Nov. 13th, **2015**, 12:00 GMT.

[2] a) H. Deacon (Gaskell, Deacon and Co.), US85370, **1868**; b) G. Leofanti, A. Marsella, B. Cremaschi, M. Garilli, A. Zecchina, G. Spoto, S. Bordiga, P. Fisicaro, G. Berlier, C. Prestipino, G. Casali, C. Lamberti, *J. Catal.* **2001**, *202*, 279–295; c) C. Lamberti, C. Prestipino, F. Bonino, L. Capello, S. Bordiga, G. Spoto, A. Zecchina, S. D. Moreno, B. Cremaschi, M. Garilli, A. Marsella, D. Carmello, S. Vidotto, G. Leofanti, *Angew. Chem. Int. Ed.* **2002**, *41*, 2341–2344; *Angew. Chem.* **2002**, *114*, 2447–2450; d) C. Rubini, M. Malentacchi (Milano, Süd Chemie), EP1020222, **2004**; e) N. B. Muddada, T. Fuglerud, C. Lamberti, U. Olsbye, *Top. Catal.* **2014**, *57*, 741–756.

[3] a) J. S. Eden (Ohio, The B. F. Goodrich Company), US4446249, **1984**; b) F. E. Van Rooijen, A. De Bruijn, J. J. Nieuwland (Amersfoort, Albemarle), US2009/0054708, **2009**.

[4] a) G. Leofanti, A. Marsella, B. Cremaschi, M. Garilli, A. Zecchina, G. Spoto, S. Bordiga, P. Fisicaro, C. Prestipino, F. Villain, C. Lamberti, *J. Catal.* **2002**, *205*, 375–381; b) N. B. Muddada, U. Olsbye, L. Caccialupi, F. Cavani, G. Leofanti, D. Gianolio, S. Bordiga, C. Lamberti, *Phys. Chem. Chem. Phys.* **2010**, *12*, 5605–5618.

[5] M. E. Jones, M. M. Olken, D. A. Hickman (Midland, The Dow Chemical Company), US6909024, **2005**.

[6] a) A. P. Amrute, C. Mondelli, M. Moser, G. Novell-Leruth, N. Lopez, D. Rosenthal, R. Farra, M. E. Schuster, D. Teschner, T. Schmidt, J. Pérez-Ramírez, *J. Catal.* **2012**, *286*, 287–297; b) M. Moser, C. Mondelli, A. P. Amrute, A. Tazawa, D. Teschner, M. E. Schuster, A. Klein-Hoffman, N. López, T. Schmidt, J. Pérez-Ramírez, *ACS Catal.* **2013**, *3*, 2813–2822; c) M. Moser, A. P. Amrute, J. Pérez-Ramírez, *Appl. Catal. B* **2015**, *162*, 602–609.

[7] a) B. de Rivas, R. López-Fonseca, J. R. González-Velasco, J. I. Gutiérrez-Ortiz, *J. Mol. Catal. A* **2007**, *278*, 181–188; b) A. S. Shalygin, L. V. Malysheva, E. A. Paukshtis, *Kinet. Catal.* **2011**, *52*, 305–315.

[8] R. Farra, S. Wrabetz, M. E. Schuster, E. Stotz, N. G. Hamilton, A. P. Amrute, J. Pérez-Ramírez, N. López, D. Teschner, *Phys. Chem. Chem. Phys.* **2013**, *15*, 3454–3465.

[9] M. Moser, G. Vilé, S. Colussi, F. Krumeich, D. Teschner, L. Szentmiklósi, A. Trovarelli, J. Pérez-Ramírez, *J. Catal.* **2015**, *331*, 128–137.

Received: November 24, 2015
Revised: December 18, 2015
Published online: January 28, 2016

